

Reducing exciton–longitudinal optical phonon coupling with increasing Mg incorporation in MgZnO powders

Ching-Ju Pan, Kuo-Feng Lin, Wei-Tse Hsu, and Wen-Feng Hsieh

Citation: [Journal of Applied Physics](#) **102**, 123504 (2007); doi: 10.1063/1.2820100

View online: <http://dx.doi.org/10.1063/1.2820100>

View Table of Contents: <http://scitation.aip.org/content/aip/journal/jap/102/12?ver=pdfcov>

Published by the [AIP Publishing](#)

Articles you may be interested in

[Effect of size on the exciton-phonon coupling strength in ZnO nanoparticles](#)

[AIP Conf. Proc.](#) **1512**, 256 (2013); 10.1063/1.4791008

[Optical properties of MgZnO alloys: Excitons and exciton-phonon complexes](#)

[J. Appl. Phys.](#) **110**, 013520 (2011); 10.1063/1.3606414

[Size dependence of exciton-phonon coupling in sol-gel ZnMgO powders](#)

[J. Appl. Phys.](#) **109**, 063526 (2011); 10.1063/1.3563574

[Analytical study on exciton-longitudinal-optical-phonon coupling and comparison with experiment for ZnO quantum wells](#)

[J. Appl. Phys.](#) **97**, 106111 (2005); 10.1063/1.1900294

[Fabrication and optical properties of ZnSe/ZnMgSSe multiple quantum wells grown by compound-source molecular beam epitaxy](#)

[J. Appl. Phys.](#) **81**, 456 (1997); 10.1063/1.364080



Re-register for Table of Content Alerts

Create a profile.



Sign up today!



Reducing exciton–longitudinal optical phonon coupling with increasing Mg incorporation in MgZnO powders

Ching-Ju Pan, Kuo-Feng Lin, Wei-Tse Hsu, and Wen-Feng Hsieh^{a)}

Department of Photonics and Institute of Electro-Optical Engineering, National Chiao Tung University, 1001 Tahsueh Road, Hsinchu 30050, Taiwan

(Received 16 September 2007; accepted 15 October 2007; published online 19 December 2007)

The coupling between exciton and longitudinal optical (LO) phonon was investigated in the use of temperature-dependent photoluminescence from $\text{Mg}_x\text{Zn}_{1-x}\text{O}$ powders prepared by a sol-gel method in the range of $0 \leq x \leq 0.05$. The exciton binding energy increases to 73 meV for 5 at. % Mg incorporated powders. The strength of exciton–LO phonon coupling was deduced from the energy shift of exciton emission with temperature variation. The increase of the exciton binding energy results from a decrease of the exciton Bohr radius that is responsible for reducing the coupling strength of exciton–LO phonon as increasing Mg content. © 2007 American Institute of Physics. [DOI: 10.1063/1.2820100]

I. INTRODUCTION

Among wide-band-gap semiconductor materials, a pronounced advantage for ZnO (3.37 eV) is its large exciton binding energy (~ 60 meV),¹ so that it has been recognized as a promising candidate to compete with GaN for the development of short-wavelength photonic devices, such as ultraviolet (UV) detectors, light-emitting diodes, and laser diodes. To fully utilize ZnO-based technologies, band gap engineering and *p*-type doping are still the remaining issues in modern optoelectronics. Li *et al.*² proposed that, using the first-principles band-structure calculations, the *p*-type dopability of ZnO can be improved by lowering the ionization energy of acceptors in ZnO by codoping acceptors with donor or isovalent atoms (e.g., Mg or Be). (Mg,Zn)O alloys have been proved feasible to realize the band gap modulation of ZnO. Additionally, MgZnO can be used as energy barrier layers of ZnO light-emitting devices and ZnO/Mg_{0.2}Zn_{0.8}O coaxial nanorod single quantum well structures for carrier confinement.^{3,4} They are also very promising materials for use as active layers in double heterostructures, e.g., Shibata *et al.*⁵ reported Zn_{1-x}Mg_xO alloys are very brilliant light emitters, even more brilliant than ZnO, particularly in the high-temperature region. Therefore, it requires a full understanding of material characteristic in MgZnO systems.

A precise knowledge of the excitonic parameters for $\text{Mg}_x\text{Zn}_{1-x}\text{O}$ alloys is important because excitons are a sensitive indicator of material quality. Especially, the exciton–phonon coupling has significant influence on the optical properties of semiconductors, such as the energy relaxation rate of excited carriers and phonon replicas of excitons in the luminescence spectra. As is well known, polar semiconductors experience a strong Fröhlich interaction that gives rise to exciton–LO phonon interaction. However, there are few attempts to study the exciton–LO phonon coupling by photoluminescence (PL) experiments in MgZnO materials. Recently, Wang *et al.*⁶ has extracted the exciton–LO phonon

coupling parameter of laser ablation prepared ZnO nanowires by resonant Raman scattering. It was found that the coupling strength of exciton–LO phonon ($\lambda_{\text{Ex-LO}}$) determined by the ratio of the second- to the first-order Raman scattering cross sections diminish with decreasing nanowire diameter. A similar observation was also found in ZnO quantum dots.⁷ Sun *et al.*,⁸ who grew ZnO/ZnMgO multi-quantum wells by laser-molecular-beam epitaxy, investigated $\lambda_{\text{Ex-LO}}$ by the temperature dependence of the linewidth of the fundamental excitonic peak from optical absorption spectra. The reduction of $\lambda_{\text{Ex-LO}}$ with decreasing well width was observed, which is consistent with the confinement-induced enhancement of the exciton binding energy (E_{XB}).

In this article, the near band-edge (NBE) luminescence properties of $\text{Mg}_x\text{Zn}_{1-x}\text{O}$ ($0 \leq x \leq 0.05$) powders prepared by a sol-gel method were comparatively analyzed with those of undoped ZnO powders by temperature-dependent PL. We found that E_{XB} of Mg-doped ZnO powders raises with increasing Mg substitution. We also investigated $\lambda_{\text{Ex-LO}}$ determined by the exciton peak shift with temperature variation on the basis of a Bose–Einstein expression. A reducing $\lambda_{\text{Ex-LO}}$ was ascribed to an increase of E_{XB} in the $\text{Mg}_x\text{Zn}_{1-x}\text{O}$ powders as the compression of the exciton Bohr radius (a_{EB}).

II. EXPERIMENTAL PROCEDURES

$\text{Mg}_x\text{Zn}_{1-x}\text{O}$ powders were synthesized using the aqueous sol prepared by stoichiometric zinc acetate dihydrate [99.5% $\text{Zn}(\text{OAc})_2 \cdot 2\text{H}_2\text{O}$, Riedel-deHaen] and magnesium acetate tetrahydrate [99.5% $\text{Mg}(\text{OAc})_2 \cdot 4\text{H}_2\text{O}$, Riedel-deHaen] (Mg/Zn=0%, 3%, and 5% in molar ratio) dissolved into methanol. The sol was dried in a furnace at 900 °C under air atmosphere for 1 h, and then slowly cooled to room temperature. Morphology of $\text{Mg}_x\text{Zn}_{1-x}\text{O}$ powders was characterized by field-emission scanning electron microscopy (JEOL-2100F). The PL measurement was made using a 40 mW He–Cd laser at wavelength of 325 nm and the emission light was dispersed by a TRIAX-320 spectrometer and de-

^{a)} Author to whom the correspondence should be addressed. Electronic mail: wfhsieh@mail.nctu.edu.tw.

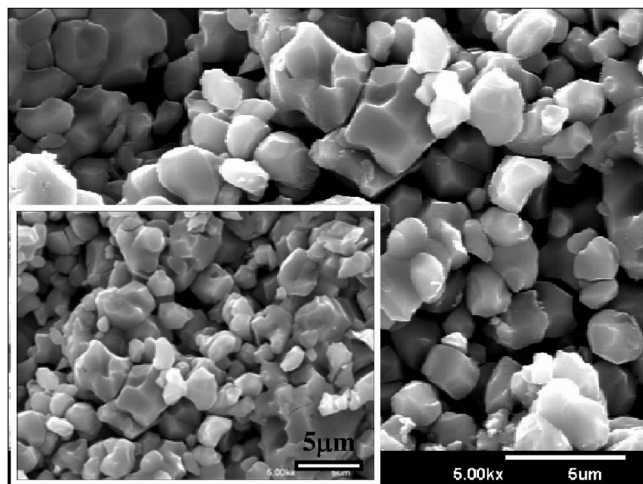


FIG. 1. SEM image of the 5% Mg sample. The inset shows the pure ZnO powders.

ected by an UV-sensitive photomultiplier tube. A closed-cycle refrigerator was used to set the temperature anywhere between 15 and 300 K.

III. RESULTS AND DISCUSSION

The average crystallite sizes of $\text{Mg}_x\text{Zn}_{1-x}\text{O}$ and ZnO powders were estimated from the scanning electron microscopy images in Fig. 1 and its inset, respectively, to be $1 \pm 0.5 \mu\text{m}$ that does not reveal quantum size effect [Bohr radius of exciton in ZnO is $\sim 2.34 \text{ nm}$ (Refs. 9 and 10)]. Accordingly, the exciton behavior was affected mainly by the incorporation of Mg. The NBE emissions of the ZnO and $\text{Mg}_{0.05}\text{Zn}_{0.95}\text{O}$ samples measured at various temperatures are shown in Figs. 2(a) and 2(b), respectively. First, we discuss the PL spectra of the undoped sample in order to comparatively assign the PL peaks of the $\text{Mg}_{0.05}\text{Zn}_{0.95}\text{O}$ powders. At $T=15 \text{ K}$ [Fig. 2(a)], the most intense PL emission line at 3.363 eV is attributed to the exciton bound to neutral donor (denoted by D^0X). On the high-energy side of the D^0X line, the A -free exciton emission (denoted by $FX_A^{n=1}$) is observed at 3.373 eV. There are two weak humps positioned at 3.388 and 3.419 eV to the even higher energy. Based on the reported energy separation of A - and B -free excitons (~ 9 – 15 meV),^{11–13} we assigned the emission centered at 3.388 eV to the B exciton transition, which is about 15 meV apart from the A exciton; and the other one hump at 3.419 eV to the first excited state $FX_A^{n=2}$ ($\sim 45 \text{ meV}$ to the $FX_A^{n=1}$ state).¹⁴ On the low-energy side of the D^0X line, the peak at 3.358 eV is attributed to biexciton (labeled BX) based on previous reports.^{15–21} Besides the broad line at the lower energy shoulder around 3.308 eV labeled as “ P ,” we also found several LO phonon replicas separated by a constant interval of 71–73 meV. The P line can be resolved into two-electron satellite,²² donor-to-acceptor pair,^{17,18} exciton-exciton scattering,¹⁶ and one LO-phonon replica of $FX_A^{n=1}$ and D^0X , respectively. With increasing temperature, the relative intensity of $FX_A^{n=1}$ increases whereas that of D^0X decreases and becomes undetectable for $T > 80 \text{ K}$. This is due to the thermal dissociation of bound exciton into free exciton at higher

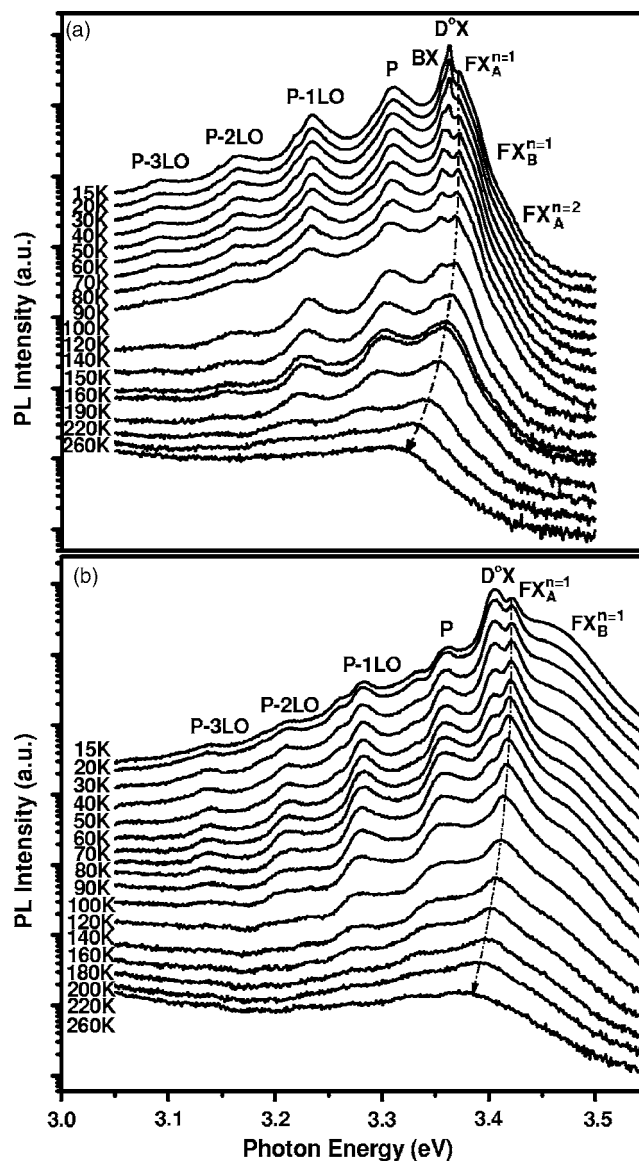


FIG. 2. Temperature dependence of PL spectra in (a) ZnO and (b) $\text{Mg}_{0.05}\text{Zn}_{0.95}\text{O}$ powders. The dashed line indicates the predicted exciton peak position.

temperature. As further increasing temperature, the A exciton, B exciton, and P line finally merge into a broad peak. At room temperature, the exciton peak position at $\sim 3.309 \text{ eV}$.

The NBE emission of the $\text{Mg}_{0.05}\text{Zn}_{0.95}\text{O}$ sample was shown in Fig. 2(b); it would evolve from that of the ZnO sample. According to the opposite temperature (RT) dependence of the relative emission intensity, the peaks at 3.422 and 3.407 eV are reasonably assigned to the $FX_A^{n=1}$ and D^0X transitions. The higher energy shoulder at 3.457 eV is related to the B exciton transition, which is 35 meV apart from the A exciton based on the reported theoretical predictions in Mg-ZnO systems.²³ The NBE peak position at RT exhibits a maximum blueshift of $\sim 74 \text{ meV}$ as 5 at. % Mg was introduced into the ZnO powders. Based on the formula $E(\text{Mg}_x\text{Zn}_{1-x}\text{O}) = E(\text{ZnO}) + 1.64x(\text{eV})$, the Mg content in the $\text{Mg}_x\text{Zn}_{1-x}\text{O}$ thin films has been determined for $0 \leq x \leq 0.2$, grown by pulsed laser deposition.²⁴ Here, $E(\text{Mg}_x\text{Zn}_{1-x}\text{O})$ and $E(\text{ZnO})$ are the NBE emission peak positions of $\text{Mg}_x\text{Zn}_{1-x}\text{O}$

TABLE I. Summary of the results of the temperature-dependent PL characterization.

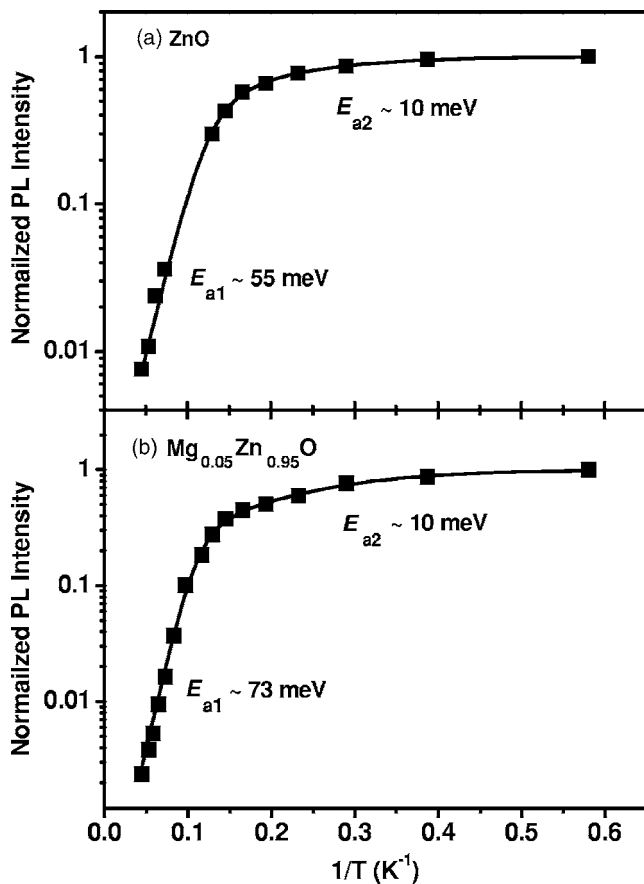
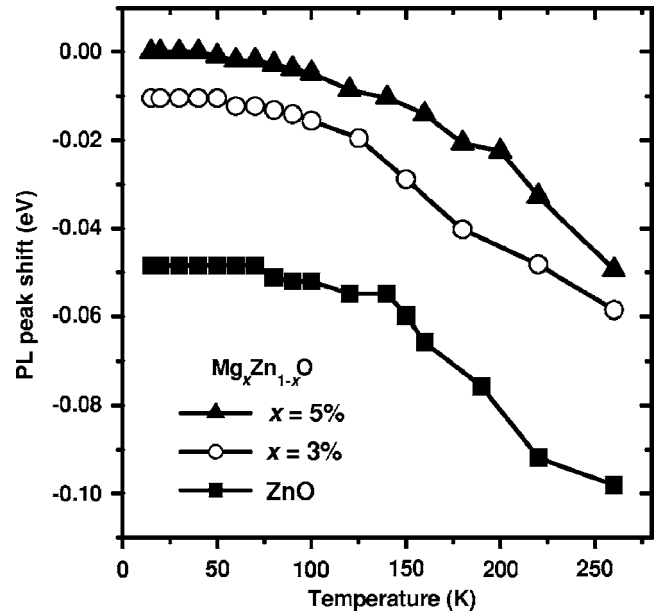
Samples: $\text{Mg}_x\text{Zn}_{1-x}\text{O}$	$x=0$	$x=3\%$	$x=5\%$
Calculated Mg content (%)	0	2.9	4.5
Exciton binding energy (meV)	55 ± 4.7	70 ± 6.7	73 ± 8.4
Exciton-LO phonon coupling strength $\lambda(\text{Mg}_x\text{Zn}_{1-x}\text{O})/\lambda(\text{ZnO})$	1	0.95	0.91

and ZnO, respectively. The calculated Mg contents of our $\text{Mg}_x\text{Zn}_{1-x}\text{O}$ alloys are shown in Table I, e.g., the molar ratio of Mg/Zn=5% was estimated to be $\sim 4.51\%$. Therefore, the blueshift of the UV emission demonstrated that the Mg ions had incorporated into the ZnO host lattice.

Figure 3 shows the peak intensity of the $FX_A^{n=1}$ emission as a function of reciprocal temperature for the undoped and Mg-doped samples. The data can be described by²⁵

$$I = I_0 [1 + a_1 \exp(-E_{a1}/kT) + a_2 \exp(-E_{a2}/kT)], \quad (1)$$

where $E_{ai}(i=1,2)$ is the activation energy in the thermal quenching process, a_1, a_2 are constants, and k is the Boltzmann constant. The curve fitting gives rise to two activation energies of approximately 55 and 11 meV for ZnO powders [Fig. 3(a)] and approximately 73 and 10 meV for $\text{Mg}_{0.05}\text{Zn}_{0.95}\text{O}$ powders [Fig. 3(b)]. In regard to the E_{a2} of ~ 10 meV, Krustok *et al.*²⁵ have reported that a low E_a may result from the temperature-dependent capture cross sections

FIG. 3. Normalized integrated intensity of (a) ZnO and (b) $\text{Mg}_{0.05}\text{Zn}_{0.95}\text{O}$ samples as a function of temperature.FIG. 4. Dependence of PL peak energy positions on temperature for the $\text{Mg}_x\text{Zn}_{1-x}\text{O}$ alloys ($x=5\%$, 3% , and 0).

of the carriers at the recombination centers, and not from a genuine thermal activation energy. Further, E_{a1} for ZnO is comparable with E_{XB} , 60 meV, for ZnO bulk, whereas that for $\text{Mg}_{0.05}\text{Zn}_{0.95}\text{O}$ is larger than 60 meV. Table I clearly shows that the binding energy of $FX_A^{n=1}$ increases markedly in samples of higher x . Therefore, this suggests that the free exciton in MgZnO alloys could survive at much higher temperatures.

It is well known the increase of E_{XB} may result from the decrease of a_{EB} or effective reduced mass. Due to the electron is more delocalized than the hole in the bulk exciton, the polar lattice experience a net negative charge in the outer regions of the exciton, whereas it experiences a net positive one in the inner regions. This charge inhomogeneity couples to the polar lattice via the Fröhlich mechanism that leads to reduce a_{EB} and to reduce the exciton-LO phonon coupling.²⁶ Thus, we further deduced the coupling strength of free exciton A with LO phonon from temperature-dependent energy shift of $FX_A^{n=1}$ as increasing Mg concentration according to the Bose-Einstein expression²⁷:

$$E(T) = E(0) - \lambda [\exp(\hbar\omega_{LO}/k_B T) - 1], \quad (2)$$

where $E(0)$ represents the emission energy of free exciton A at $T=0$ K, $\hbar\omega_{LO}=72$ meV is the LO phonon energy, and λ is a proportional coefficient which reflects a change in the exciton-LO phonon interaction.

Figure 4 depicts the PL-peak energy shift as a function of the temperature with different Mg concentrations. Notice that we had set the PL-peak energy position to zero for $\text{Mg}_{0.05}\text{Zn}_{0.95}\text{O}$ powders at 15 K. By fitting the experimental data for all the $\text{Mg}_x\text{Zn}_{1-x}\text{O}$ and ZnO powders from $T=15$ to 260 K with Eq. (2), the exciton-LO phonon coupling of each $\text{Mg}_x\text{Zn}_{1-x}\text{O}$ sample are compared with ZnO powder by taking the average ratios, $\lambda_{\text{Mg}_x\text{Zn}_{1-x}\text{O}}/\lambda_{\text{ZnO}}$, which are listed in Table I clearly show decreasing as more Mg incorporation. Even though a_{EB} and λ are not directly proportional, there is

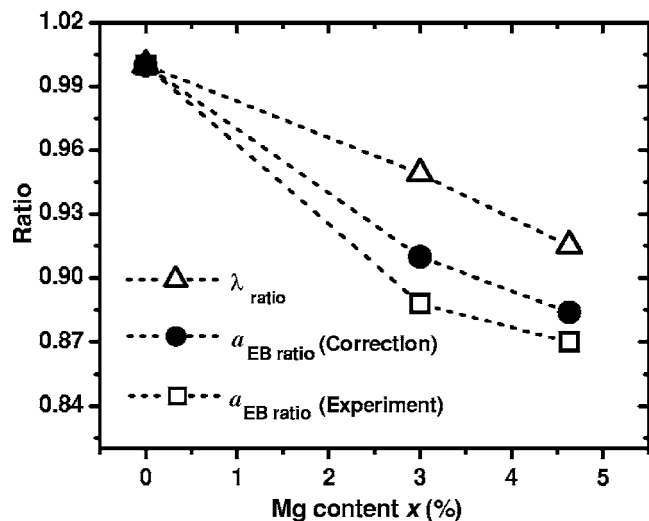


FIG. 5. Coupling strength of the exciton-LO phonon given as the average ratio $\lambda_{\text{ratio}} = \lambda_{\text{Mg}_x\text{Zn}_{1-x}\text{O}} / \lambda_{\text{ZnO}}$. For comparison, the diminution of a_{EB} for experiment and correction is also given as $a_{\text{EB ratio}} = a_{\text{EB Mg}_x\text{Zn}_{1-x}\text{O}} / a_{\text{EB ZnO}}$.

a relation: If a_{EB} reduces λ will also reduce. Assuming that the Mg-doped ZnO powders have almost the same effective electron and hole masses as the undoped ZnO powders due to a small amount of Mg^{2+} substitution for Zn^{2+} , we calculated a_{EB} from E_{XB} . The correlation between λ and a_{EB} normalized to ZnO powders are shown in Fig. 5 with open triangles and squares, respectively. Besides, the solid dots are obtained by the modified effective masses, which were corrected from MgZnO electronic band structure using semi-empirical tight-binding approach sp^3 model^{28,29} and virtual-crystal approximation method.³⁰ Therefore, a contraction of a_{EB} will make it less polar thereby reducing the coupling to LO phonons. The results show that relaxation by means of LO phonon becomes the less important as the more Mg incorporation. Consequently, we attribute this reducing coupling effect to increase in E_{XB} with raising Mg mole fraction up to 5% of $\text{Mg}_x\text{Zn}_{1-x}\text{O}$ powders. The reduction of $\lambda_{\text{Ex-LO}}$ has to take into account for the MgZnO-based excitonic device performance in which carrier relaxation to the exciton ground state is a crucial parameter.

IV. CONCLUSIONS

The temperature-dependent NBE PL spectra of $\text{Mg}_x\text{Zn}_{1-x}\text{O}$ powders within the range $0 \leq x \leq 0.05$ were measured from 15 K to RT. The RT excitonic transition energy showed being tuned by ~ 74 meV toward the UV range upon more Mg substitution. We deduced experimentally E_{XB}

showing elevation in powders up to 5% Mg substitution. The reduction of $\lambda_{\text{Ex-LO}}$ may originate from a diminution in a_{EB} making the exciton less polar, which could be explained by the dopant-induced increase of E_{XB} .

ACKNOWLEDGMENTS

This work was supported by the National Science Council of Taiwan under Contract No. NSC-96-2628-E-009-018-MY3. The authors would like to thank NSC for the award of a fellowship, and S. Yang for SEM characterization.

- ¹K. Hümmer, Phys. Status Solidi B **56**, 249 (1973).
- ²J. Li, S. H. Wei, S. S. Li, and J. B. Xia, Phys. Rev. B **74**, 081201 (2006).
- ³J. H. Lim, C. K. Kang, K. K. Kim, I. K. Park, D. K. Hwang, and S. J. Park, Adv. Mater. **18**, 2720 (2006).
- ⁴J. Y. Bae, J. Yoo, and G. C. Yi, Appl. Phys. Lett. **89**, 173114 (2006).
- ⁵H. Shibata, H. Tampono, K. Matsubara, A. Yamada, K. Sakurai, S. Ishizuka, S. Niki, and M. Sakai, Appl. Phys. Lett. **90**, 124104 (2007).
- ⁶R. P. Wang, G. Xu, and P. Jin, Phys. Rev. B **69**, 113303 (2004).
- ⁷H. M. Cheng, K. F. Lin, H. C. Hsu, and W. F. Hsieh, Appl. Phys. Lett. **88**, 261909 (2006).
- ⁸H. D. Sun, T. Makino, Y. Segawa, M. Kawasaki, A. Ohtomo, K. Tamura, and H. Koinuma, Appl. Phys. Lett. **78**, 2464 (2001).
- ⁹R. T. Senger and K. K. Bajaj, Phys. Rev. B **68**, 045313 (2003).
- ¹⁰K. F. Lin, H. M. Cheng, H. C. Hsu, L. J. Lin, and W. F. Hsieh, Chem. Phys. Lett. **409**, 208 (2005).
- ¹¹D. C. Reynolds, D. C. Look, B. Jogai, C. W. Litton, G. Cantwell, and W. C. Harsch, Phys. Rev. B **60**, 2340 (1999).
- ¹²C. Boemare, T. Monteiro, M. J. Soares, J. G. Guilherme, and E. Alves, Physica B (Amsterdam) **308-310**, 985 (2001).
- ¹³D. G. Thomas, J. Phys. Chem. Solids **15**, 86 (1960).
- ¹⁴A. Teke, U. Ozgur, S. Dogan, X. Gu, H. Morkoc, B. Nemeth, J. Nause, and H. O. Everitt, Phys. Rev. B **70**, 195207 (2004).
- ¹⁵H. D. Sun, T. Makino, Y. Segawa, M. Kawasaki, A. Ohtomo, K. Tamura, and H. Koinuma, Appl. Phys. Lett. **78**, 3385 (2001).
- ¹⁶A. Yamamoto, K. Miyajima, T. Goto, H. J. Ko, and T. Yao, J. Appl. Phys. **90**, 4973 (2001).
- ¹⁷B. P. Zhang, N. T. Binh, Y. Segawa, K. Wakatsuki, and N. Usami, Appl. Phys. Lett. **83**, 1635 (2003).
- ¹⁸B. P. Zhang, N. T. Binh, Y. Segawa, Y. Kashiwaba, and K. Haga, Appl. Phys. Lett. **84**, 586 (2004).
- ¹⁹S. W. Kim, S. Fujita, and S. Fujita, Appl. Phys. Lett. **86**, 153119 (2005).
- ²⁰X. Q. Zhang, Z. G. Yao, S. H. Huang, I. Suemune, and H. Kumano, J. Appl. Phys. **99**, 063709 (2006).
- ²¹C. J. Pan, K. F. Lin, and W. F. Hsieh, Appl. Phys. Lett. **91**, 111907 (2007).
- ²²A. Teke, U. Ozgur, S. Dogan, X. Gu, H. Morkoc, B. Nemeth, J. Nause, and H. O. Everitt, Phys. Rev. B **70**, 195207 (2004).
- ²³R. Schmidt *et al.*, Appl. Phys. Lett. **82**, 2260 (2003).
- ²⁴M. Lorenz *et al.*, Appl. Phys. Lett. **86**, 143113 (2005).
- ²⁵J. Krustok, H. Collan, and K. Hjelt, J. Appl. Phys. **81**, 1442 (1997).
- ²⁶J. J. Shiang, S. H. Risbud, and A. P. Alivisatos, J. Chem. Phys. **98**, 8432 (1993).
- ²⁷T. Makino, C. H. Chia, N. T. Tuan, Y. Segawa, M. Kawasaki, A. Ohtomo, K. Tamura, and H. Koinuma, Appl. Phys. Lett. **76**, 3549 (2000).
- ²⁸A. Kobayashi, O. F. Sankey, S. M. Volz, and J. D. Dow, Phys. Rev. B **28**, 935 (1983).
- ²⁹K. F. Lin, C. J. Pan, and W. F. Hsieh, Appl. Phys. A (submitted).
- ³⁰D. W. Jenkins and J. D. Dow, Phys. Rev. B **39**, 3317 (1989).